# Extratropical signature of the quasi-biennial oscillation

Alexander Ruzmaikin and Joan Feynman
Jet Propulsion Laboratory, California Institute of Technology, Pasadena, California, USA

Xun Jiang and Yuk L. Yung
Department of Geological and Planetary Sciences, California Institute of Technology, Pasadena, California, USA

Received 24 August 2004; revised 29 December 2004; accepted 24 February 2005; published 14 June 2005.

[1] Using the assimilated data from the National Centers for Environmental Prediction (NCEP) reanalysis, we show that the extratropical signature of the tropical quasi-biennial oscillation (QBO) is seen mostly in the North Annular Mode (NAM) of atmospheric variability. To understand the extratropical manifestation of the QBO, we discuss two effects that have been suggested earlier: (1) The extratropical circulation is driven by the QBO modulation of the planetary wave flux, and (2) the extratropical circulation is driven by the QBO-induced meridional circulation. We found that the first effect is seen in wave 1 in the beginning of winter and in wave 2 in the end of winter. The QBO-induced circulation affects midlatitude regions over the entire winter. To investigate the QBO-NAM coupling, we use an equation that relates the stream function of the meridional circulation and the polar cap averaged temperature, which is a proxy for the NAM index. In addition to the annual $\Omega_a$ and the QBO frequency $\Omega_Q$ the spectrum of its solutions indicates the satellite frequencies at $\Omega_a \pm \Omega_Q$.

**Citation:** Ruzmaikin, A., J. Feynman, X. Jiang, and Y. L. Yung (2005), Extratropical signature of the quasi-biennial oscillation, *J. Geophys. Res.*, *110*, D11111, doi:10.1029/2004JD005382.

## 1. Introduction

[2] Observational studies show that the quasi-biennial oscillation (QBO), which originates in the tropical stratosphere, affects midlatitude and polar atmospheric dynamics [*Baldwin et al.*, 2001]. However the physical mechanism of this remote influence is not well understood.

[3] One possible effect involves the QBO alteration of the Eliassen-Palm (EP) planetary wave flux that drives the middle and high-latitude dynamics. As originally found by *Holton and Tan* [1980], the polar night winds are weaker during the east phase of the QBO and stronger during its west phase. Holton and Tan suggested the following mechanism to explain this tropical-extratropical connection: During the east phase of the QBO the boundary surface separating westerly and easterly zonal winds is shifted into the winter hemisphere by about 10°. This narrows the channel for the propagation of planetary waves, which can only travel through westerly wind, and redirects their flux toward the winter pole [*Andrews et al.*, 1987]. However, the data available in 1980 were not sufficient to justify this mechanism. Later, *Dunkerton and Baldwin* [1991] using 25 years of National Meteorological Center data found that the EP flux integrated over middle to high latitudes was somewhat, but apparently not statistically significantly, higher during the east than during the west QBO. These authors concluded that they ''cannot state that planetary wave fluxes were exclusively a ''cause'' of the extratropical QBO''.

[4] In the 1990s another effect, which involves the QBO-induced meridional circulation, was proposed [*Kinnersley*, 1999; *Kinnersley and Tung*, 1999]. Earlier, this circulation was believed to be confined to the tropics in the form of a two-cell structure symmetrically localized about the equator [*Plumb and Bell*, 1982]. Then it was shown that the planetary waves in the winter hemisphere strongly affect this QBO-induced circulation thus making it season-dependent [*Gray and Dunkerton*, 1990]. Using a simple zonally averaged isentropic model *Kinnersley* [1999] and *Kinnersley and Tung* [1999] showed that when the planetary wave drag, which is effective in winter, was applied to the zonal wind the winter cell is greatly strengthened and expanded into the winter hemisphere. The QBO-induced circulation becomes asymmetric with respect to the equator, penetrating to middle and high latitudes and thus directly influencing the extratropical circulation. The modeling also indicated that the Holton-Tan effect could still be responsible for the QBO signal near the winter pole.

[5] Note that both effects involve the planetary waves because there can be no meridional circulation without wave driving. In the Holton-Tan effect the QBO directly affects the waveguide, whereas in the second effect the wave flux affects the QBO-induced meridional circulation. Thus these effects can be considered as two parts of one, more general mechanism.

[6] Here we investigate these two effects of the QBO influence on the extratropics using extensive data analysis that employs the assimilated data from the National Centers


0148-0227/05/2004JD005382$09.00

for Environmental Prediction (NCEP) reanalysis in Northern Hemisphere in 1958–2002. In section 2, we demonstrate that the spatial pattern of the extratropical anomalies in geopotential heights induced by the QBO is very much the same as the annular mode of the atmospheric variability in the winter hemisphere. In section 3 we evaluate the statistical significance of the Holton-Tan effect. In section 4, we test the influence of the QBO-induced circulation by constructing the stream functions of the meridional circulation during the east and west QBO time periods from the NCEP reanalysis data. To further elucidate this point we also carry out a statistical test, in which the periods of the east and west QBO are randomly mixed. In section 5, we complement the data analyses with simple theoretical considerations based on a relationship between the meridional circulation, the planetary wave flux, and the North Annular Mode.

## 2. Spatial Imprint of the QBO in the Extratropics

[7] What is the spatial signature of the effect of the QBO in the middle to high latitude region of the Northern Hemisphere? It was shown earlier [*Dunkerton and Baldwin*, 1991] that the anomalous zonal wind related to the QBO changes direction at about 40°–50° latitude. The spatial, dipole-type structure of this anomaly bears a remarkable resemblance to the spatial structure of the North Annular Mode (NAM) of atmospheric variability discovered later [*Thompson and Wallace*, 1998]. The NAM is the first Empirical Orthogonal Function (EOF) of geopotential heights. It is confined to 20°–90° with a sign change at 40°–50°. The NAM extends from the top of the stratosphere through the troposphere to sea level accounting for 22% of the variance in geopotential heights at sea level and for a higher percentage of the variance in the stratosphere (50% at 50 hPa) [*Thompson and Wallace*, 1998; *Baldwin and Dunkerton*, 1999]. The principal components of the mode are called the NAM index. The mode is believed to be excited by nonlinear interplay between the planetary waves and mean zonal wind [*Limpasuvan and Hartmann*, 2000]. A number of earlier data analyses indicated that the NAM index is correlated with the QBO phase [*Naito and Hirota*, 1997; *Caughlin and Tung*, 2001; *Ruzmaikin and Feynman*, 2002; *Hu and Tung*, 2002a].

[8] To directly study the structure of the QBO-induced anomaly in geopotential heights we employ the NCEP reanalysis monthly data for 1958–2002. We use the composite of the difference in geopotential heights calculated for the east and west QBO periods. Other effects, which are contributing to the anomalies independently of the QBO, such the ENSO, are suppressed in these composites. In Figure 1 we plot a composite of the difference in geopotential heights calculated for the east and west QBO time periods in four winter months (November through February). A two-sign structure similar to the NAM is clearly seen in Figure 1, indicating that EOFs higher than the NAM make relatively small contribution to geopotential height anomalies influenced by the QBO.

[9] To further confirm the nature of the QBO anomaly we follow the definition of the NAM and plot in Figure 2 the difference in the first EOFs of geopotential heights calculated separately for the east and west QBO time periods. A comparison of Figures 1 and 2 shows that they are very similar except for regions that are close to the equatorial boundary (<30°). As we will show in section 4, the QBO-induced circulation is strong in this region. We suggest that these deviations are due to the QBO-induced meridional circulation.

[10] Testing the statistical significance of this difference, as well as the differences in the wave flux and stream functions studied in the next sections, requires statistical methods suitable for the small number ($N < 20–30$) of monthly data points, which are available for the composite differences. Usually the standard $t$ test is applied. However the application of the $t$ test requires that the data be normally distributed, which is not the case with data used in our study. It is known that the distribution function of the geopotential height anomalies produced by the planetary waves is strongly non-Gaussian [*Pawson and Kubitz*, 1996]. To circumvent this problem we apply the bootstrap method, which can be used for any distribution function of the data [*Efron and Tibshirani*, 1993]. (For control purposes we also applied the $t$ test, which in this case gave estimates close to those produced by the bootstrap method.)

[11] In the bootstrap method [*Efron and Tibshirani*, 1993], the observed set of data of size N is considered as a sample taken from an unknown distribution. The composite we calculate is the mean value of this observed set. If a large number of data points were available then the sum of data divided by N would be a good approximation to the mean of the unknown distribution (according the central limit theorem). The observed distribution of a relatively small number of data points can, however, be utilized for estimation of the underlying unknown probability distribution function that can then be used for estimation of the mean value. Introducing an empirical distribution function, defined by assigning a 1/N probability to each of the observed data points, allows the generation of many samples from the data points. The generation of the bootstrap samples consists of repeated random resampling of data that includes rearrangement of the data points as well as the use of the same data points more than once. For example, data points (1, 2, 3, 4, 5) could be resampled as (1, 1, 3, 3, 2). For each resampled data set a new map similar to one in Figure 1 is calculated. This is repeated $n$ times (here, 1000). Now each grid cell (pixel) of the figure plane contains $n$ values, which we sort into increasing order. Then the range of values from the $m$th to the $(n - m)$th gives an estimate of the confidence interval, for example, 99% for $m = 5$ and 95% for $m = 25$. If the random samples were drawn from a normal (Gaussian) distribution the 95% confidence level would correspond to the familiar $2\sigma$ standard error. If the observed values, in our case the differences obtained from actual data, do not belong to this interval, that is, they are outliers, the observed differences are statistically significant at the selected confidence level. The pixels statistically significant at the 95% level are shaded in Figure 1. For all months, the effect is statistically significant at this level in the upper stratosphere and at a lower statistical level in low stratosphere and in the troposphere.

[12] The statistical significance above is evaluated locally, and on the assumption that all data points are time independent and there is no interdependence between spatial pixels. In other words, we assumed that each data point is

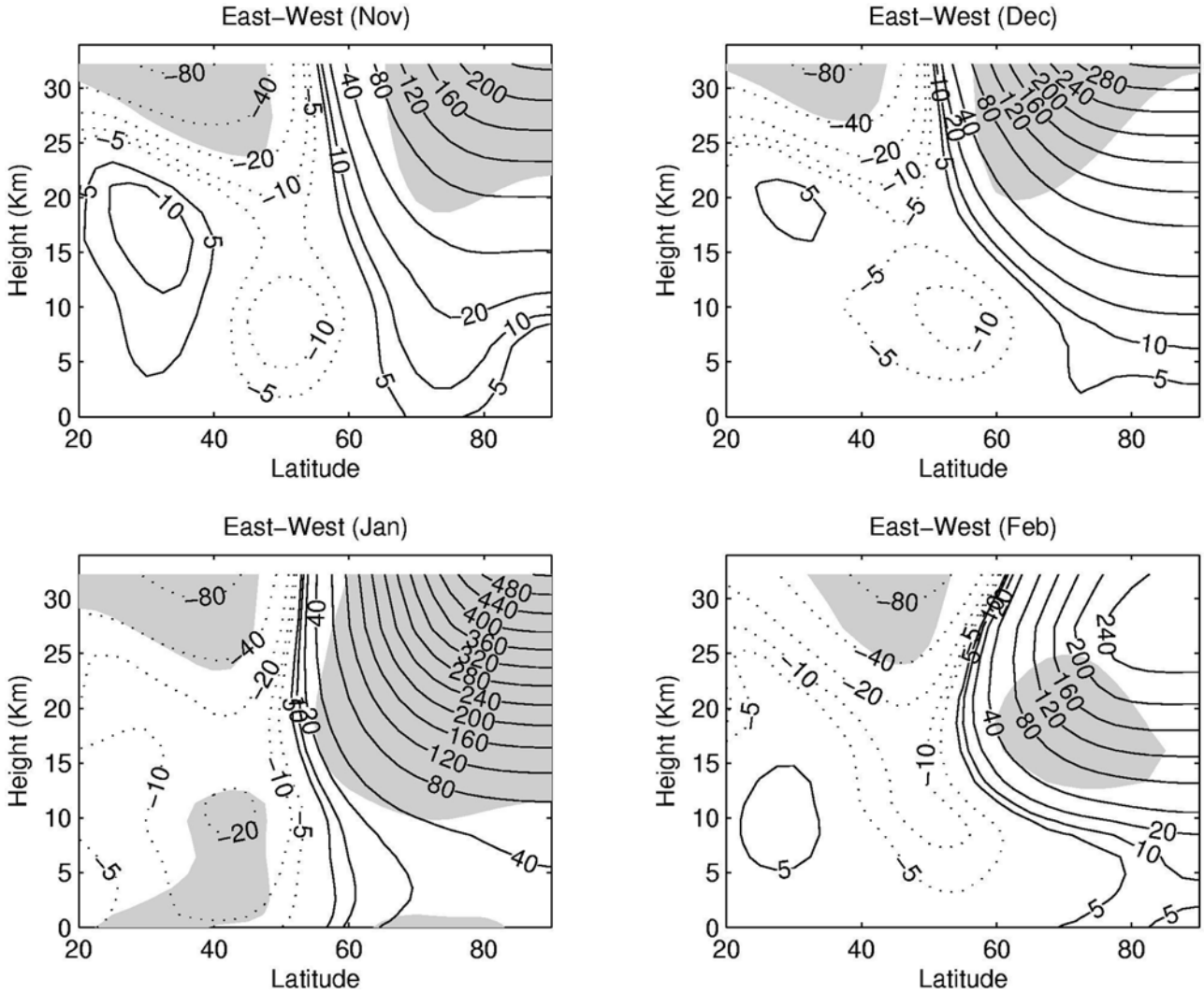


**Figure 1.** Difference in the east-west QBO composites of the geopotential heights (in meters) constructed using winter monthly data from NCEP reanalysis for 1958–2002. (East QBO periods are defined as times when the tropical zonal wind at 40 hPa is lower than $-3$ m s$^{-1}$. West QBO periods are defined as times when the tropical zonal wind is higher than 3 m s$^{-1}$.) There are $29 \times 17 = 493$ points in the latitude-potential temperature domain. The 17 vertical levels range from 1000 to 10 hPa. The latitudinal resolution is 2.5. The areas statistically significant at the 95% level are shaded. The percentages of statistically significant areas relative to whole area are 12.2% (November), 10% (December), 41.4% (January), and 10.1% (February).

representative for reconstruction of the distribution. Because the amount of data is limited, a global (collective) significance should be evaluated as well to guarantee that the outcome is not a result of a small but lucky set of data. Time and/or spatial correlations may seriously influence the evaluation of the collective significance by reducing the effective degrees of freedom [*Livezey and Chen*, 1983]. The simplest idea to estimate the collective statistical significance, suggested by *Livezey and Chen* [1983], is to treat the estimate of statistical significance in each pixel as an outcome of a coin-tossing trial with ''head'' corresponding to passing say the 95% test (probability of getting it by random is smaller than 0.05) and 'tail' to not passing the test. The sample of pixels can be treated as N independent coins and the result of tossing can be considered as a collection of N independent tests. Then the binomial (two-outcome) distribution for the percent of significant areas at a given N can be utilized. The graph of the area determined by the threshold probability (0.05) and plotted as a function of N [*Livezey and Chen*, 1983, Figure 3] allows an estimate of the effective degrees of freedom ($N^*$) needed to pass the collective test. In our data analysis of geopotential heights we use $N = 29 \times 17 = 493$ spatial pixels in latitude-height domain and 15 to 22 points for each winter month during the east or west QBO periods. If there is no correlation between the pixels, then the critical percent of significant tests passed at 95% level can be evaluated from Figure 3 of *Livezey and Chen* [1983]. (We made a rough estimate of autocorrelations to check that there is no time correlation between the subsequent years for each winter month in the geopotential height anomalies for the east-west QBO differences we used.)

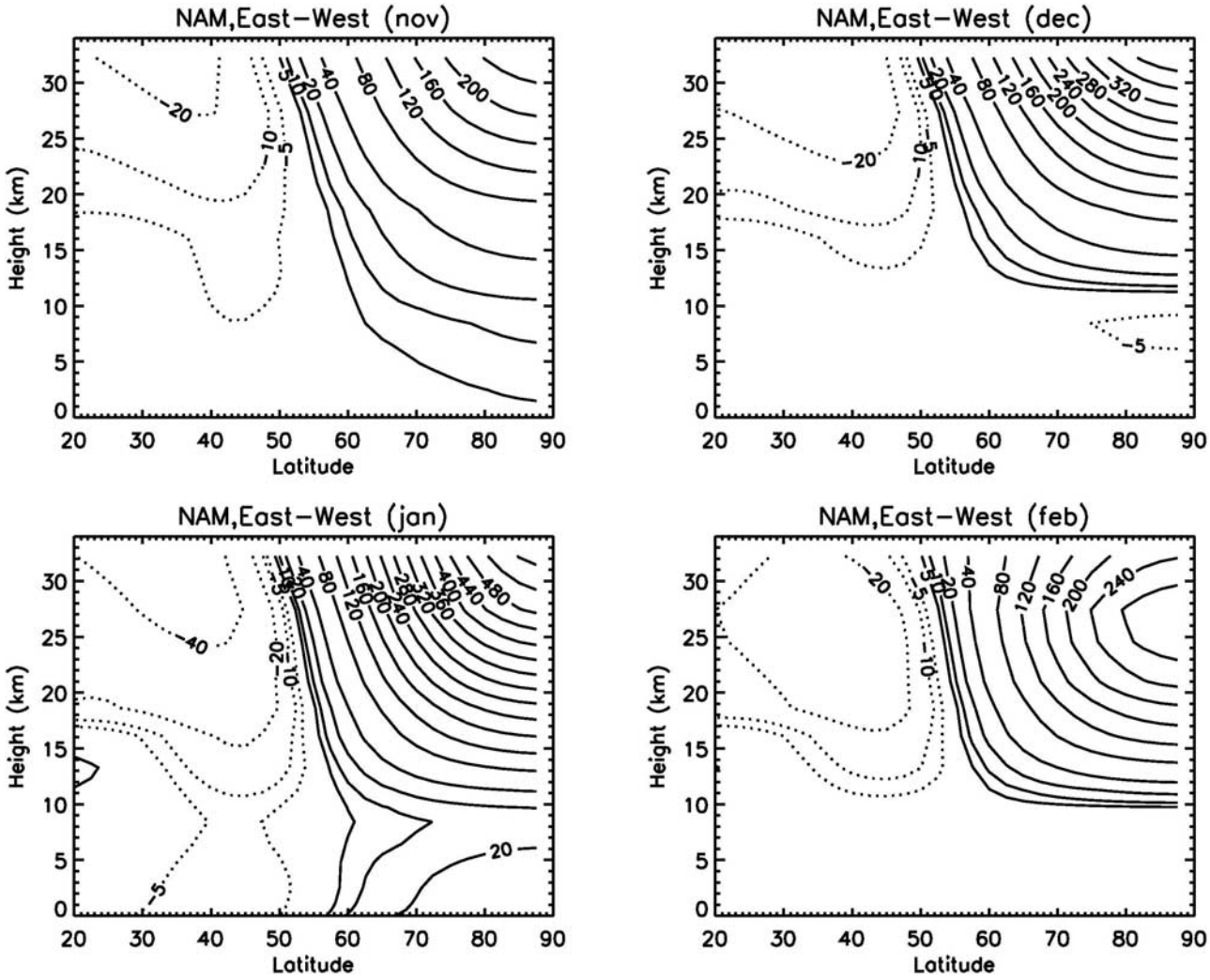


**Figure 2.** Difference in the first EOFs of geopotential heights (NAMs) calculated for the east-west QBO time periods. The numbers on the contours are in meters.

[13] To evaluate the collective significance in this way we first calculate the percentage of areas statistically significant at the 95% level (Figure 1, shaded area). For 493 independent pixels the critical level determined from Figure 3 of *Livezey and Chen* [1983] is only about 7%. This means that with more than 10% of the shaded area in each winter month in Figure 1 we easily pass the collective significance test in this approximation. However because the QBO effect manifests itself as the NAM (a coherent pattern) there is a strong interdependence between the pixels, which effectively reduces the degrees of freedom N used above. For a crude estimate of the reduction in the degrees of freedom we may use the fact that the NAM explains 22–50% of variability dependent of the atmospheric height. The reduction of N in half increases the critical percent to about 7.5% level, which is still sufficient for the collective statistical significance of our results.

[14] Because the NAM can be excited not only by the QBO but also by many other forcings, we should check whether the reported effect is caused by the QBO or occurred by chance. For this purpose we run the following collective statistical test. Instead of using the real dates for the east and west QBO periods we randomly mixed the QBO dates. After each such random mix, repeated 1000 times, we calculated the percent of statistically significant (at 95% level) area. The histograms of these 1000 areas are plotted in Figure 3. We see that January result is above the 95% level of significance. The results for other winter months are significant at lower level.

## 3. Quasi-Biennial Modulation of Planetary Wave Fluxes in the Northern Hemisphere Winter

[15] Let us test the Holton-Tan proposition for the QBO influence on the EP flux. For that purpose we calculate the EP fluxes for the east and west QBO periods using the NCEP reanalysis data for 1958–2002. The east and west phases are defined using the sign of the tropical QBO winds at 40 hPa. We employ the $z$ component of the EP flux calculated from the NCEP reanalysis 1958–2002 data. Note that this component and the integrated flux used by *Dunkerton and Baldwin* [1991] have the same time dependence. We also separated wave 1 and wave 2 contributions, as suggested earlier by *Hu and Tung* [2002a].

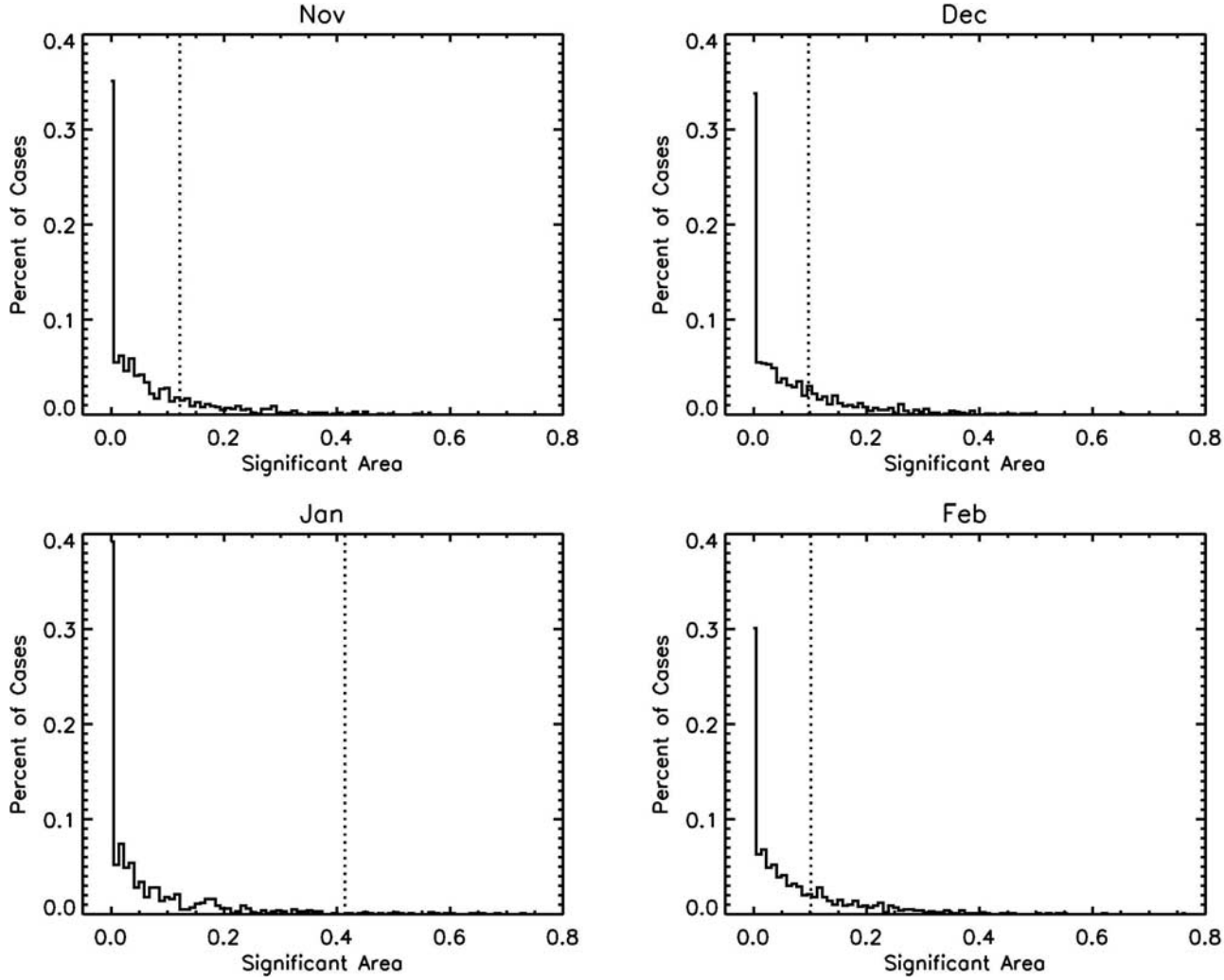


**Figure 3.** Results of a collective statistical significance test of the anomalies shown in Figure 1. The test is based on the random mix of the QBO dates. The distributions of the areas statistically significant at the 95% level in the randomized tests are shown for four winter months. The vertical dotted lines mark the percentage of statistically significant areas obtained with real dates as shown in Figure 1.

[16] Figure 4 shows the composite of the $F_z$ fluxes for the planetary wave number 1 at (a) 20 hPa and (b) 200 hPa at 60°N latitude in the winter. These heights and the latitudes are shown to directly compare with the results by *Dunkerton and Baldwin* [1991]. Figure 5 shows the fluxes for wave number 2. In agreement with Dunkerton and Baldwin, who used a smaller data set and could not demonstrate the statistical significance, the flux of wave 1 in the beginning of winter during the east QBO exceeds the flux during the west QBO. In mid winter the west QBO flux exceeds the east QBO flux for wave 1, and there is no significant difference between these fluxes in February and March. There is a difference in the fluxes for the wave number 2 at the end of winter (in February and March). The statistical significance was evaluated using the bootstrap method. We found that the flux differences are significant at 95% ($2\sigma$) level. The ratio of the differences between the curves normalized by the standard deviation indicates that levels of significance at the beginning of winter in the stratosphere and the troposphere for wave 1, and in February–March in the stratosphere for wave 2 are actually better than $3\sigma$.

## 4. QBO-Induced Anomaly in the Meridional Circulation

[17] Consider now the role of the meridional circulation induced by the QBO. To compare the modeling results by *Kinnersley* [1999] and *Kinnersley and Tung* [1999] with observations we investigate the meridional circulation using the 1958–2002 NCEP reanalysis data. We employ the monthly averaged mass stream function defined on isentropic surfaces [*Jiang et al.*, 2004]. The algorithm describing the calculation of the stream function is given in the cited paper. Here we calculate the stream functions separately for the east and west QBO time periods. Note that the QBO-induced meridional circulation has opposite directions during the east and west QBO. During the east (west) QBO the air rises (sinks) at equator and sinks (rises) at midlatitudes.

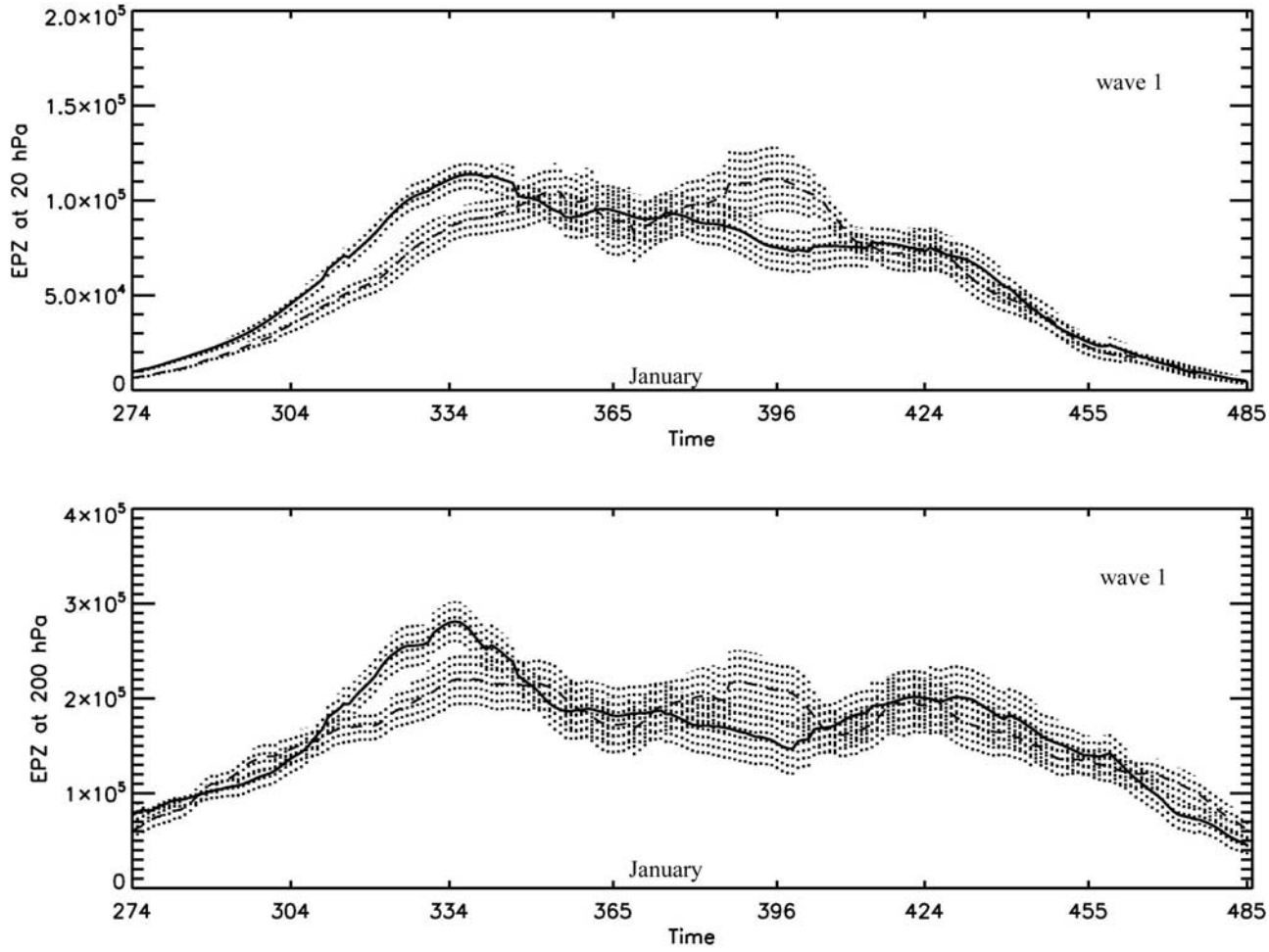


**Figure 4.** Composite $F_z$ flux carried by wave 1 for the east QBO (solid curve) and west QBO (dashed curve) at 20 and 200 hPa, at 60°N. The time interval (in calendar day of the year) extends from October to April. The area marked by dotted lines corresponds to error bars at the 95% level of statistical significance. The flux is measured in units of kg $s^2$.

[18] To eliminate the mean Brewer-Dobson circulation driven by the planetary wave flux during both phases of the QBO we take the east-west QBO difference of the stream functions. The difference is plotted in Figure 6. In accord with the modeling [*Kinnersley*, 1999; *Kinnersley and Tung*, 1999], we see that the observed QBO-induced meridional circulation penetrates to 50° and higher latitudes in the Northern Hemisphere.

[19] The shaded parts of Figure 6 are statistically significant at 95% level. The statistical significance is evaluated by the bootstrap method. The collective statistical significance is evaluated as has been discussed in relation to the geopotential heights in Figure 1 but with higher confidence because the percentages of statistically significant at 95% level (shaded) areas relative to whole area are 25.2% (November), 24.1% (December), 22.9% (January), and 20.2% (February).

[20] As described in section 3, to check if the anomaly circulation shown in Figure 6 is due to the QBO we randomized the east and west QBO dates and, after each random mix repeated 1000 times, we calculated the percent of statistically significant (at 95% level) area for four winter months. The histograms of the areas, which are statistically significant at this level are plotted in Figure 7. We see that in this case all winter months results clearly pass this test at the 95% level. The reason the stream function anomalies show better statistical significance compared with the anomalies in geopotential heights is probably due to the fact that the stream function is driven by dissipative processes only whereas geopotential heights are subjected to a wide spectrum of adiabatic and nonadiabatic disturbances.

## 5. Discussion

[21] Let us discuss possible relationships between the residual meridional circulation, the EP flux and the NAM.

[22] A local thermal or mechanical forcing of a compressible rotating fluid can affect regions remote from the forcing, as first shown by *Eliassen* [1951] and further developed by *Plumb* [1982] and *Garcia* [1987]. The quasi-geostrophic balance itself is restored instantly (on a timescale of the inverse of the Coriolis parameter) but the support of stationary circulation against the forcing requires meridional motions or an adjustment of the temperature–zonal wind distribution. By prescribing the sources of heat and mechanical torques these authors

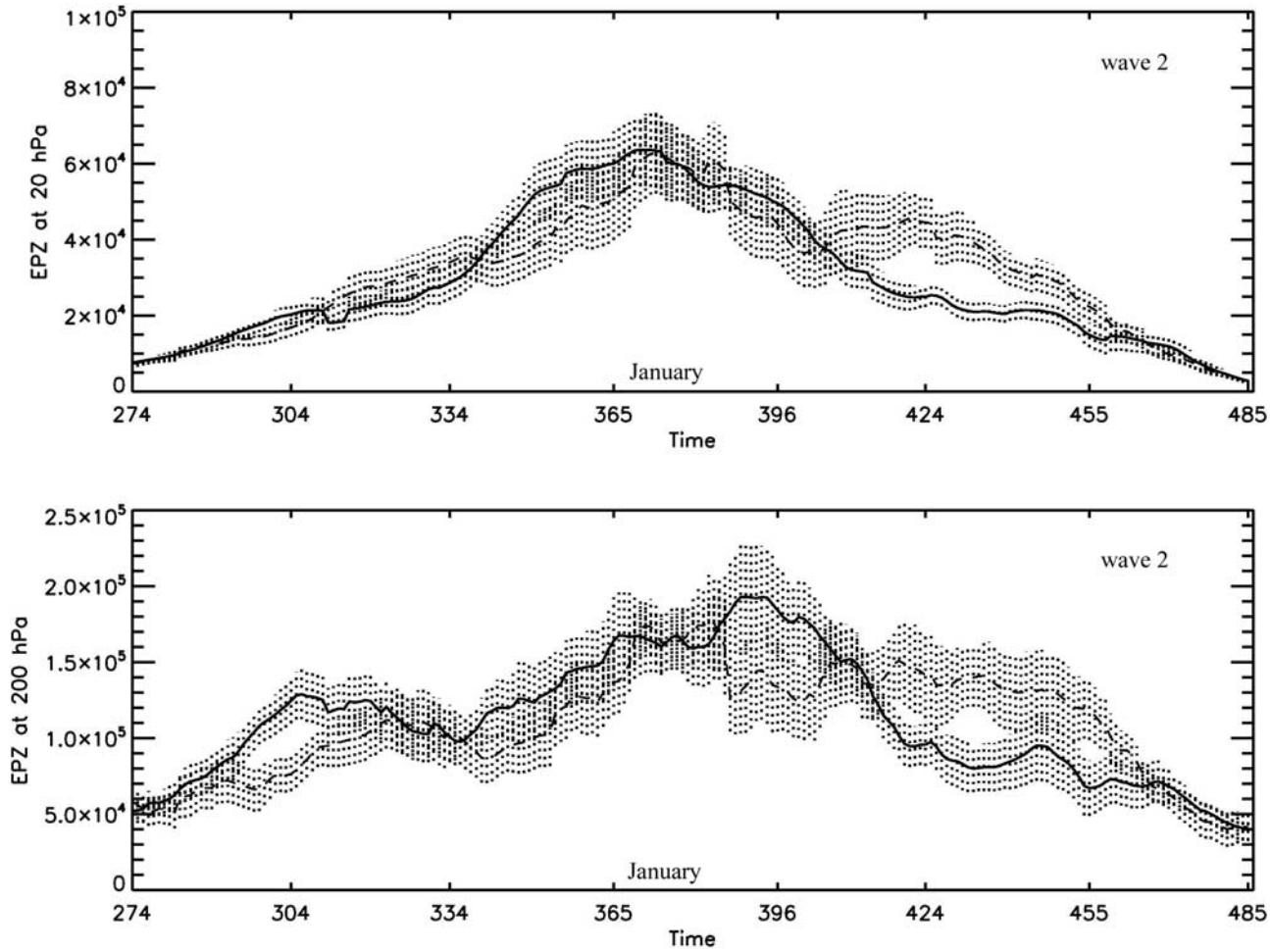


**Figure 5.** Same as in Figure 4 but for wave 2.

reduced the problem to a linear elliptic equation for the stream function of the meridional circulation, the right side of which is determined by the heat and mechanical sources.

[23] This ''electrostatic'' approach, while elegant, is based on assumptions that the sources of heat and angular momentum are prescribed (thus excluding nonlinear feedbacks), and that the circulation is stationary (thus excluding the time variability of the circulation). The assumption that the circulation is stationary was somewhat relaxed by *Garcia* [1987], who considered a periodic forcing under the condition that the system response has the same frequency as the forcing. This limited extension does not, however, allow a consideration of the more realistic situation, for example when the seasonal, EP flux, and QBO variations vary simultaneously with different frequencies.

[24] To address this nonstationary problem we employ here a simple differential equation that relates the meridional circulation and the polar cap averaged temperature [*Newman et al.*, 2001; *Hu and Tung*, 2002b]. The NAM index, defined as the principal component of the first EOF of geopotential heights, is strongly anticorrelated with the polar temperatures [*Gillett et al.*, 2001]. For example, the correlation coefficient between the temperature and the NAM index is $-0.87$ in January and $-0.73$ in April at 70 hPa. We will use here the polar cap averaged temperature as a proxy for the NAM index.

[25] The residual meridional velocity is defined as [*Andrews et al.*, 1987]

$$v^* = v - \frac{1}{\rho_0}\frac{\partial}{\partial z}\left(\frac{\rho_0\overline{v'\theta'}}{\theta_{0z}}\right), w^* = w + \frac{1}{a\cos\phi}\frac{\partial}{\partial\phi}\left(\frac{\cos\phi\overline{v'\theta'}}{\theta_{0z}}\right), \tag{1}$$

where $\theta$ is the potential temperature, $\theta_{0z} = d\theta/dz$, $\rho_0(z)$ is the density, $f$ is the Coriolis parameter, and $a$ is the Earth's radius. The velocity ($v^*$, $w^*$) corrects ($v$, $w$) for the drag produced by the $z$ component of the EP flux ($F_z = \rho_0 f\overline{v'\theta'}/\theta_{0z}$). The continuity equation

$$\frac{1}{a\cos\phi}\frac{\partial(\rho_0 v^*\cos\phi)}{\partial\phi} + \frac{\partial\rho_0 w^*}{\partial z} = 0 \tag{2}$$

implies the existence of a stream function

$$\rho_0 v^*\cos\phi = -\frac{\partial\Psi}{\partial z}, \quad \rho_0 w^* a\cos\phi = \frac{\partial\Psi}{\partial\phi}. \tag{3}$$

[26] The mechanism by which the QBO affects extratropics is essentially nonsteady. It involves the seasonal, and the QBO periodicities as well as periodicities produced in the process. A simple way to investigate these time depen-

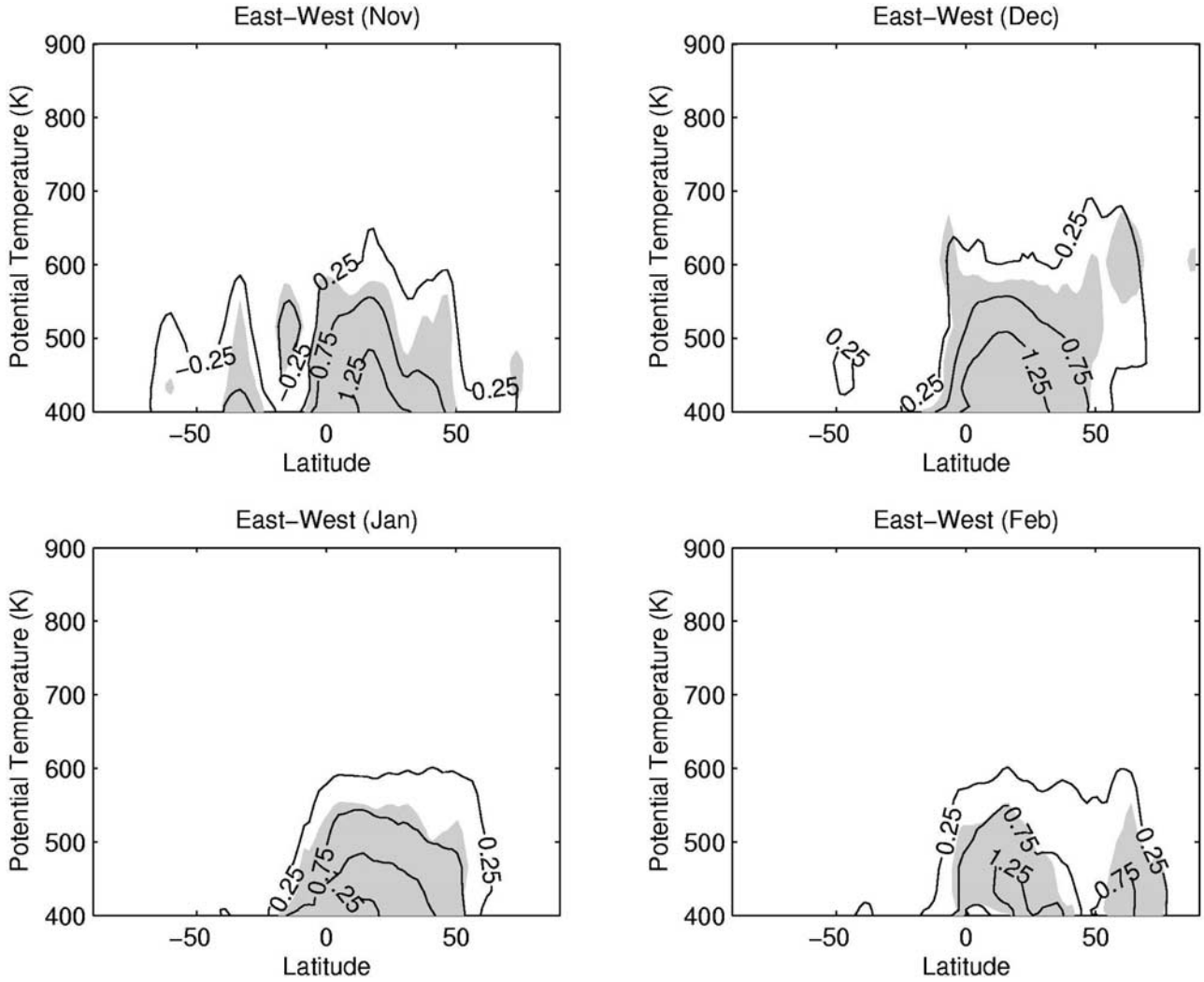


**Figure 6.** Differences between the composites of the east QBO and west QBO mass stream functions on isentropic surfaces. The stream function is measured in $10^9$ kg s$^{-1}$. There are $94 \times 6 = 564$ points in the latitude-potential temperature domain. The six vertical levels used in calculations are 900, 605, 516, 466, 432, and 407 K. (For better orientation and a rough comparison with the standard pressure height scale we assessed (using January 1980 data at 60°N latitude) that these potential temperature levels correspond to pressure heights 7.4, 25.2, 43.7, 63.1, 82.8, and 103.2 hPa, respectively.) The areas statistically significant at the 95% level are shaded. The percentages of the shaded areas relative to the whole area are 25.2% (November), 24.1% (December), 22.9% (January), and 20.2% (February).

dencies comes through a relationship between the stream function and temperature. The zonal-mean temperature in the extratropical regions is governed by the equation [*Andrews et al.*, 1987]

$$\frac{\partial \theta}{\partial t} + w^* \theta_{0z} = Q_0 - \alpha\theta. \tag{4}$$

The right-hand side includes the shortwave heating ($H$) and the infrared cooling $B + \alpha\theta$ with $Q_0 = H - B$ and $\alpha$ being the Newton cooling coefficient.

[27] The cap-averaged equation (4), that is, area-weighted from a latitude $\phi$ to the pole $\phi = \pi/2$, has a simple form [*Newman et al.*, 2001; *Hu and Tung*, 2002b]

$$\frac{\partial \bar{\theta}}{\partial t} + \alpha\bar{\theta} = \frac{\theta_{0z}\Psi|_\phi}{a\rho_0(1-\sin\phi)} + \bar{Q}_0, \tag{5}$$

where the bar means

$$\bar{\theta} = \frac{\int_\phi^{\pi/2} \theta \cos\varphi d\varphi}{\int_\phi^{\pi/2} \cos\varphi d\varphi} = \frac{\int_\phi^{\pi/2} \theta \cos\varphi d\varphi}{1-\sin\phi},$$

and the value of the stream function is taken at the boundary of the averaging area. Using a $\phi$ that exceeds the latitude separating the positive and negative spatial parts of the NAM (45°–50°), we can find the changes in the NAM if variations of $\Psi|_\phi$ and the radiative average $\bar{Q}_0$ are known. The solution of equation (5) is

$$\bar{\theta} = \bar{\theta}_0 e^{-\alpha t} + e^{-\alpha t}\int_0^t e^{\alpha t'}\left(\frac{\theta_{0z}\Psi|_\phi}{\rho_0(1-\sin\phi)} + \bar{Q}_0\right)dt'. \tag{6}$$

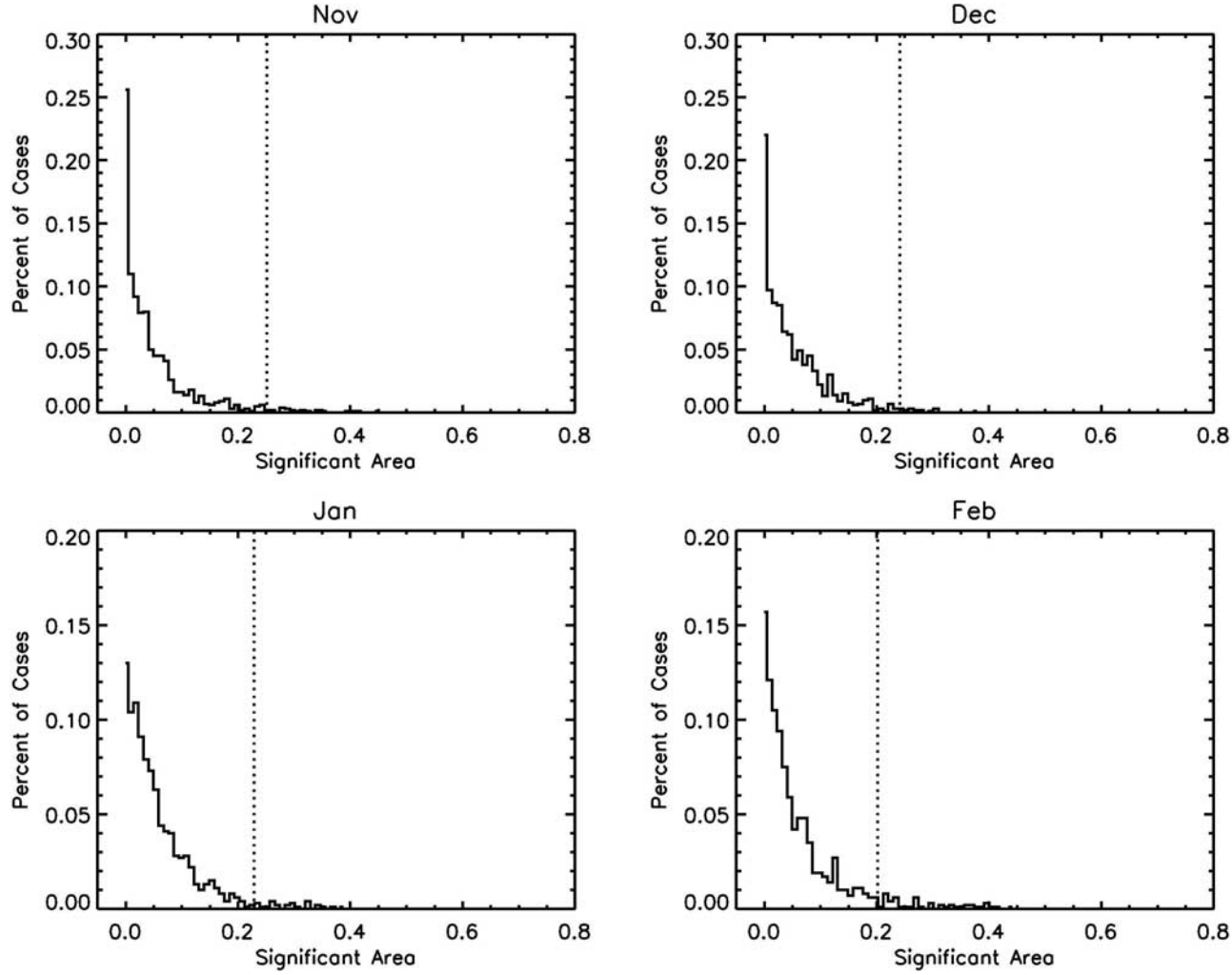


**Figure 7.** Results of a collective statistical significance test of the anomalies shown in Figure 6. The test is based on the random mix of the QBO dates. The distributions of the areas statistically significant at the 95% level are shown for four winter months. The dotted vertical lines mark the percentage of statistically significant areas obtained with real dates as shown in Figure 6.

[28] Hence the polar cap averaged temperature at time t is determined by the stream function in all previous times. The near-polar behavior of the cap-averaged temperature deserves special attention, because the factor $(1 - \sin\phi)^{-1}$ in (6) diverges as $(\pi/2 - \phi)^{-2}$ when $\phi \to \pi/2$. However no singularity occurs because $\Psi = \int_{\phi}^{\pi/2} w^* \cos\phi d\phi \approx w^*(1 - \sin\phi))$ in the same limit so the ratio of $\Psi$ to $(1 - \sin\phi))$ in (6) is constant.

[29] Consider now the time behavior of the polar cap temperature assuming that the time dependence of the stream function is given, that is, we treat $\bar{\theta}$ as "passive scalar" neglecting its back action on the meridional circulation. The integrand in the right side of the equation (8) undergoes an annual cycle, which we simulate with $\cos\Omega_a t$, where $\Omega_a = 1/12$ months$^{-1}$. We can approximate the amplitude and annual cycle in the thermal source as

$$Q = Q_0 \cos(\Omega_a t), \tag{7}$$

where $Q_0 = 10^{-4}\exp[-(z - 50\text{ km})/15\text{ km}]^2(\sin\phi)^{-5/2}$ K/s [*Garcia*, 1987]. As we found in the previous two sections, both parts of the stream function (the meridional circulation and the planetary wave drag) are modulated by the QBO. To simulate this we present the stream function in the form

$$\Psi = \Psi_0\big(1 + \delta\cos\big(\Omega_Q t + \beta\big)\big)(C + \cos\Omega_a t), \tag{8}$$

where $\Psi_0$ is the magnitude of the stream function, $\Omega_Q \approx 1/28$ months$^{-1}$ and $\beta$ are the QBO frequency and phase. This simple presentation describes an oscillator with annual frequency $\Omega_a$, the amplitude of which is offset by constant $C$ and modulated by the low-frequency $\Omega_Q$. The term $C$ accounts for the Brewer-Dobson circulation. The amplitude and phase of the QBO modulation $(\delta, \beta)$ can be estimated from data such as used in the previous sections. To simplify the situation we do not take into account the annual cycle of the radiative terms in equation (4), in particular the annual cycle in the damping parameter $\alpha$ [*Newman and Rosenfeld*, 1997].

[30] Substituting these time dependencies into (6) we immediately see that the cap-averaged temperature (the proxy for the NAM index) has five time-dependent terms. The first is proportional to $\exp(-\alpha t)$ and decays as $1/\alpha$. The

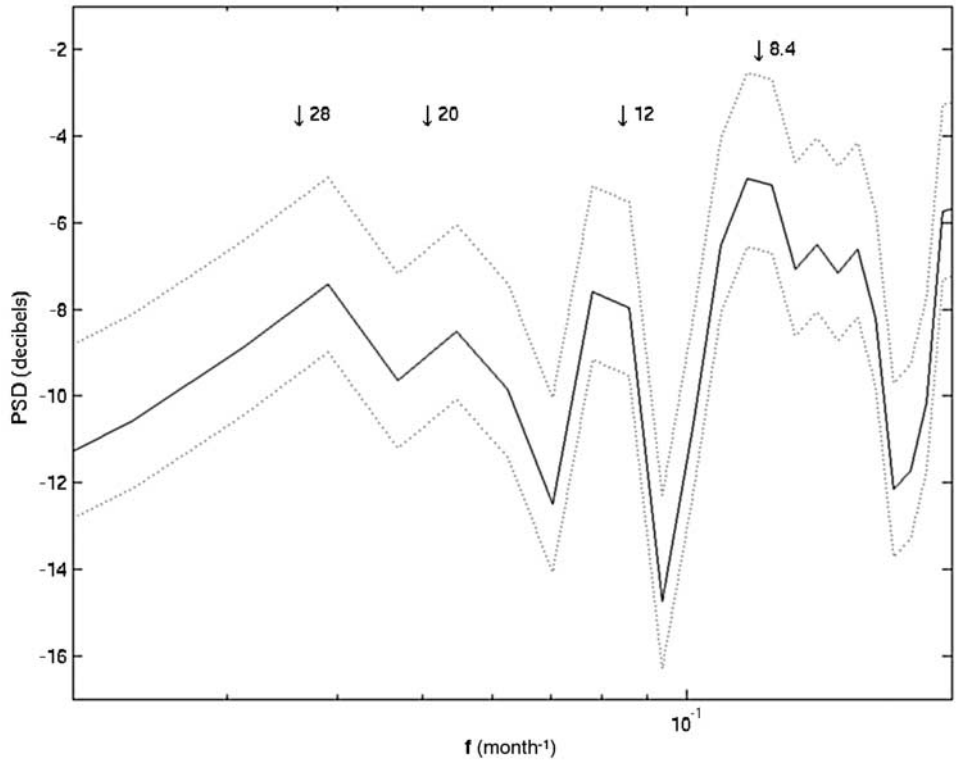


**Figure 8.** Spectrum of the polar temperature at 20 hPa. The power spectral density (in decibels) is estimated using Welch's method from MATLAB. Arrows mark the positions of the QBO (28 months) and satellite frequencies expected from equation (5) (inverse 20 months and 8.4 months) as well as the (partly filtered) annual frequency. The confidence intervals at $1\sigma$ are indicated by dotted lines.

second term is periodic with the annual frequency, $\Omega_a$. It has an amplitude proportional to $1/\alpha$ and is phase-shifted relative to the driver by $\tan^{-1}(\alpha/\Omega_a)$. Using $1/\alpha = 30$ days we find that this phase shift corresponds to a time delay of the polar temperature response to the annual variation of the driver of about 2.8 months. This rough estimate qualitatively agrees (but slightly exceeds) the observational estimate by *Newman et al.* [2001], who found that the polar temperature at 100 hPa in March is the best correlated with the $z$ component of the EP flux taken in earlier months (January–February). The third term is periodic with the QBO frequency $\Omega_Q$. The fourth and fifth terms are periodic with frequencies $\Omega_a - \Omega_Q$ and $(\Omega_a + \Omega_Q)$. The last two frequencies are comparable with the 20 month and 8.4 month periodicities found in the data analysis of the ozone transport in the midlatitudes [*Tung and Yang*, 1994a, 1994b]. As indicated by these authors and clear demonstrated by *Hamilton* [1995] who separated equator symmetric and antisymmetric transport of ozone, the dynamics associated with these frequencies is related to the seasonal cycle.

[31] Figure 8 shows the spectrum of the polar temperature calculated using the NCEP reanalysis monthly data in 1948–2002. The observed spectrum indicates all the above frequencies and thus tends to support the theoretical prediction.

## 6. Conclusions

[32] We demonstrated that the mechanism of the QBO influence on the extratropics operates mostly through the NAM, although there are deviation from the NAM in the low-latitude regions. The mechanism involves the QBO modulation of the vertical component of the planetary wave flux (Holton-Tan effect) and the QBO-induced meridional circulation [*Kinnersley*, 1999; *Kinnersley and Tung*, 1999]. The QBO modulation of the planetary wave flux affects the extratropics in the beginning of winter for wave 1 and in the end of winter for wave 2. The QBO-induced circulation affects extratropics during entire winter. It penetrates into the midlatitudes because of the seasonal variation of the planetary wave flux (strong in winter, weak in summer). The NAM index displays strong annual variation with a phase delay relative to the changes in the planetary flux. It also shows a weaker signal at the QBO period and at periods defined by the sum and difference of the annual and QBO frequencies.

[33] **Acknowledgments.** This research was carried out in part at the Jet Propulsion Laboratory, California Institute of Technology, under a contract with the National Aeronautics and Space Administration and was funded through the internal Research and Technology Development program. We are grateful to David Camp and Run-Lie Shia for their generous help in this study. We thank three anonymous reviewers for their critical and helpful comments.

## References

Andrews, D. G., J. R. Holton, and C. B. Leovy (1987), *Middle Atmosphere Dynamics*, 489 pp., Elsevier, New York.

Baldwin, M. P., and T. J. Dunkerton (1999), Propagation of the Arctic Oscillation from the stratosphere to the troposphere, *J. Geophys. Res.*, *104*, 30,937–30,946.

Baldwin, M. P., et al. (2001), The quasi-biennial oscillation, *Rev. Geophys.*, *39*, 179–229.

Caughlin, K., and K. K. Tung (2001), QBO signal found at the extratropical surface through northern annular modes, *Geophys. Res. Lett.*, *28*, 4563–4566.

Dunkerton, T. J., and M. P. Baldwin (1991), Quasi-biennial modulation of planetary wave fluxes in the Northern Hemisphere winter, *J. Atmos. Sci.*, *48*, 1043–1061.

Efron, B., and R. J. Tibshirani (1993), *An Introduction to the Bootstrap*, *Monogr. Stat. Appl. Probab.*, vol. 57, CRC Press, Boca Raton, Fla.

Eliassen, A. (1951), Slow thermally or frictionally controlled meridional circulation in a circular vortex, *Astrophys. Norv.*, *5*, 19–59.

Garcia, R. R. (1987), On the mean meridional circulation of the middle atmosphere, *J. Atmos. Sci.*, *44*, 3599–3609.

Gillett, N., P. M. Baldwin, and M. R. Allen (2001), Evidence for nonlinearity in observed stratospheric circulation changes, *J. Geophys. Res.*, *106*, 7891–7901.

Gray, L. J., and T. J. Dunkerton (1990), The role of the seasonal cycle in the quasi-biennial oscillation of ozone, *J. Atmos. Sci.*, *47*, 2429–2451.

Hamilton, K. (1995), Comment on "Global QBO in circulation and ozone. Part I: Reexamination of observational evidence," *J. Atmos. Sci.*, *52*, 1834–1838.

Holton, J. R., and H.-C. Tan (1980), The influence of the equatorial quasi-biennial oscillation on the global circulation at 50 mb, *J. Atmos. Sci.*, *37*, 2200–2208.

Hu, Y., and K. K. Tung (2002a), Tropospheric and equatorial influences on planetary-wave amplitude in the stratosphere, *Geophys. Res. Lett.*, *29*(2), 1019, doi:10.1029/2001GL013762.

Hu, Y., and K. K. Tung (2002b), Interannual and decadal variations of planetary wave activity, stratospheric cooling, and Northern Hemisphere annular mode, *J. Clim.*, *15*, 1659–1673.

Jiang, X., C. D. Camp, R. Shia, D. Noone, C. Walker, and Y. L. Yung (2004), Quasi-biennial oscillation and quasi-biennial oscillation-annual beat in the tropical total column ozone: A two-dimensional model simulation, *J. Geophys. Res.*, *109*, D16305, doi:10.1029/2003JD004377.

Kinnersley, J. S. (1999), Seasonal asymmetry of the low- and middle-latitude QBO circulation anomaly, *J. Atmos. Sci.*, *56*, 1140–1153.

Kinnersley, J. S., and K. K. Tung (1999), Mechanisms for the extratropical QBO in circulation and ozone, *J. Atmos. Sci.*, *56*, 1942–1962.

Limpasuvan, V., and D. L. Hartmann (2000), Wave-maintained annular modes of climate variability, *J. Clim.*, *13*, 4414–4429.

Livezey, R. E., and W. Y. Chen (1983), Statistical field significance and its determination by Monte Carlo techniques, *Mon. Weather Rev.*, *111*, 46–59.

Naito, Y., and I. Hirota (1997), Interannual variability of the northern winter stratospheric circulation related to the QBO and the solar cycle, *J. Meteorol. Soc. Jpn.*, *75*, 925–937.

Newman, P. A., and J. E. Rosenfeld (1997), Stratospheric thermal damping times, *Geophys. Res. Lett.*, *24*, 433–436.

Newman, P. A., E. R. Nash, and J. E. Rosenfeld (2001), What controls the temperature of the Arctic stratosphere during the spring?, *J. Geophys. Res.*, *106*, 19,999–20,010.

Pawson, S., and T. Kubitz (1996), Climatology of planetary waves in the Northern Hemisphere, *J. Geophys. Res.*, *101*, 16,987–16,996.

Plumb, R. A. (1982), Zonally symmetric Hough modes and meridional circulations in the middle atmosphere, *J. Atmos. Sci.*, *39*, 983–991.

Plumb, R. A., and R. C. Bell (1982), A model of the quasi-biennial oscillation on the equatorial beta plane, *Q. J. R. Meteorol. Soc.*, *108*, 335–352.

Ruzmaikin, A., and J. Feynman (2002), Solar influence on a major mode of atmospheric variability, *J. Geophys. Res.*, *107*(D14), 4209, doi:10.1029/2001JD001239.

Thompson, D. W. J., and J. M. Wallace (1998), The Arctic Oscillation signature in the wintertime geopotential height and temperature fields, *Geophys. Res. Lett.*, *25*, 1297–1300.

Tung, K. K., and H. Yang (1994a), Global QBO in circulation and ozone, part I: Reexamination of observational evidence, *J. Atmos. Sci.*, *51*, 2699–2707.

Tung, K. K., and H. Yang (1994b), Global QBO in circulation and ozone, part II: A simple mechanistic model, *J. Atmos. Sci.*, *51*, 2708–2717.

J. Feynman and A. Ruzmaikin, Jet Propulsion Laboratory, California Institute of Technology, 4800 Oak Grove Dr., Pasadena, CA 91109, USA. (aruzmaik@pop.jpl.nasa.gov)

X. Jiang and Y. L. Yung, Department of Geological and Planetary Sciences, California Institute of Technology, Mail Stop 150-21, Pasadena, CA 91125, USA.